Food Control 119 (2021) 107494

Contents lists available at ScienceDirect

Food Control

journal homepage: www.elsevier.com/locate/foodcont

Effect of physicochemical factors and use of milk powder on milk rennet-coagulation: Process understanding by near infrared spectroscopy and chemometrics

Lorenzo Strani [a], Silvia Grassi [a,*], Cristina Alamprese [a], Ernestina Casiraghi [a], Roberta Ghiglietti [b], Francesco Locci [b], Nicolò Pricca [b], Anna De Juan [c]

[a] Department of Food, Environmental, and Nutritional Sciences (DeFENS), Università degli Studi di Milano, Via G. Celoria 2, 20133, Milan, Italy
[b] CREA-ZA, Research Centre for Animal Production and Aquaculture, Via A. Lombardo 11, 26900, Lodi, Italy
[c] Chemometrics Group. Department of Chemical Engineering and Analytical Chemistry, Universitat de Barcelona, Diagonal 645, 08028, Barcelona, Spain

ARTICLE INFO

Keywords:
Milk powder
Coagulation
Near infrared spectroscopy
Multivariate curve resolution
Alternating least squares
Rheological properties

ABSTRACT

The effect of physicochemical factors and use of skim milk powder on milk rennet-coagulation was investigated combining near infrared (NIR) spectroscopic monitoring and Multivariate Curve Resolution - Alternating Least Squares (MCR-ALS). Coagulum formation has been studied by reference approaches (Formagraph and fundamental rheology) and with NIR spectroscopy on unaltered reconstituted milk samples, pasteurized samples, samples with calcium chloride addition and samples of reconstituted milk mixed with fresh milk. The MCR-ALS models successfully described the process evolution, explaining more than 99.9% of variance. The MCR-ALS profiles revealed to be significantly directly correlated with Formagraph and rheological data ($p < 0.001$) and allowed assessing the significant effect ($p < 0.05$) of the milk powder type on the coagulation occurrence and the non-significance ($p > 0.05$) of the $CaCl_2$ concentration level added and the heat treatment applied. The MCR-ALS models calculated for the coagulation trials of pasteurized skimmed milk mixed with reconstituted milk samples highlighted shorter coagulation times with the increasing of reconstituted milk amount (from 4.3-6.6 min to 2–5 min). Profiles extracted from MCR-ALS models developed for a wide range of coagulation conditions proved to be suitable non-destructive, non-invasive and on-line tools to evaluate the rennet-induced coagulation of reconstituted milks.

1. Introduction

From an economic and technological point of view, skimmed milk powder (SMP) is pivotal for countries in which milk production is scarce or absent due to climatic and high cost issues (Kjaergaard-Jansen, 1990; Lelievret, Shaker, & Taylor, 1991; Omar & Buchheim, 1983; Písecký, 2005), but also for top milk-producing countries. Indeed, SMP addition is relevant for protein content standardization in milk intended for cheesemaking (Lin, Kelly, O'Mahony, & Guinee, 2017; Písecký, 2005) as well as for the production cost saving if fresh milk price increases (Papadatos, Berger, Pratt, & Barbano, 2002).

SMPs differ mainly due to the technology used for their production. In particular, depending on the severity of the heat treatment and on the milk pH, the dehydration process affects the extent of whey protein denaturation and the binding of denatured whey protein to the casein micelles (Singh & Waungana, 2001). These changes affect cheese processing and the use of reconstituted skim milk may cause problems, such as longer coagulation time, slower syneresis, and formation of weaker or finer curd (Singh & Waungana, 2001). These effects may modify typical texture, ripening and functionality of the resulting cheese (Gulati et al., 2019; Rynne, Beresford, Kelly, & Guinee, 2004; Singh & Waungana, 2001). Several studies (Gastaldi, Pellegrini, Lagaude, & de la Fuente, 1994; Lucey, Gorry, & Fox, 1994; Sandra, Ho, Alexander, & Corredig, 2012; Singh & Waungana, 2001; Udabage, McKinnon, & Augustin, 2000) have revealed that the adverse effects of heat treatment on rennet coagulation can be overcome, to some extent, by adding calcium

* Corresponding author. Address: Via Celoria 2, 20133, Milan, Italy.
E-mail addresses: lorenzo.strani@unimi.it (L. Strani), silvia.grassi@unimi.it (S. Grassi), cristina.alamprese@unimi.it (C. Alamprese), ernestina.casiraghi@unimi.it (E. Casiraghi), roberta.ghiglietti@crea.gov.it (R. Ghiglietti), francesco.locci@crea.gov.it (F. Locci), nicolo.pricca@gmail.com (N. Pricca), anna.dejuan@ub.edu (A. De Juan).

https://doi.org/10.1016/j.foodcont.2020.107494
Received 21 April 2020; Received in revised form 16 July 2020; Accepted 17 July 2020
Available online 25 July 2020

Table 1
Description of the samples used for the coagulation trials.

Sample ID	Number of replicates	Country	Manufacturing company	Powder type	$CaCl_2$ (g/L)	Sample pasteurization	Percentage of fresh milk
Effect of milk powder type and added $CaCl_2$ on coagulation time							
EPI 18	2	France	EPI ingredients	Low heat	0.018	no	0
EPI 35	2	France	EPI ingredients	Low heat	0.035	no	0
Lactalis 18	2	France	Lactalis	Medium-heat	0.018	no	0
Lactalis 35	2	France	Lactalis	Medium-heat	0.035	no	0
Rucker 18	2	Germany	Rucker	Instant	0.018	no	0
Rucker 35	2	Germany	Rucker	Instant	0.035	no	0
Safivo 18	2	France	Safivo	Medium-heat	0.018	no	0
Safivo 35	2	France	Safivo	Medium-heat	0.035	no	0
SCA 18	2	Spain	Lafuente	Medium-heat	0.018	no	0
SCA 35	2	Spain	Lafuente	Medium-heat	0.035	no	0
SIA 18	2	Ireland	Glanbia	Instant	0.018	no	0
SIA 35	2	Ireland	Glanbia	Instant	0.035	no	0
Effect of pasteurization on coagulation							
Skimmed P	2	CREA-ZA	–	Skimmed fresh milk	0.035	yes	100
Skimmed NP	2	CREA-ZA	–	Skimmed fresh milk	0.035	no	100
EPI P	2	France	EPI ingredients	Low heat	0.035	yes	0
EPI NP	2	France	EPI ingredients	Low heat	0.035	no	0
SCA P	2	Spain	Lafuente	Medium-heat	0.035	yes	0
SCA NP	2	Spain	Lafuente	Medium-heat	0.035	no	0
Effect of addition of reconstituted milk to fresh milk on coagulation							
EPI 40	3	France	EPI ingredients	Low heat	0.035	no	60
EPI 60	3	France	EPI ingredients	Low heat	0.035	no	40
SCA 40	3	Spain	Lafuente	Medium-heat	0.035	no	60
SCA 60	3	Spain	Lafuente	Medium-heat	0.035	no	40

chloride ($CaCl_2$). The higher concentration of Ca^{2+} ions probably reduces electrostatic resistance between casein micelles, thus increasing aggregation (Singh & Waungana, 2001).

In cheesemaking, clotting time and coagulum firmness are commonly measured by Formagraph (Pretto et al., 2011). Several works have recently demonstrated also the usefulness of fundamental and empirical rheology in monitoring properties of rennet-induced milk gels (Grassi, Strani, Casiraghi, & Alamprese, 2019; Han, Mei, Li, Xu, & Wang, 2019; Kern, Bähler, Hinrichs, & Nöbel, 2019; Nassar et al., 2020; Salvador, Arango, & Castillo, 2019). However, these analytical systems are quite intrusive and unsuitable for the in-line/on-line monitoring of commercial cheesemaking (O'Callaghan, O'Donnell, & Payne, 2002). On the contrary, near infrared (NIR) spectroscopy has been recognized as a reliable analytical technology for the assessment of several quality parameters of a wide range of dairy products (IDF, 2019). Moreover, NIR spectroscopy, coupled with the use of specific chemometric tools, proved to be successful also for the evaluation of physical changes (Cabassi, Profaizer, Marinoni, Rizzi, & Cattaneo, 2013; Marinoni, Monti, Barzaghi, & de la Roza-Delgado, 2013; Strani, Grassi, Casiraghi, Alamprese, & Marini, 2019), thus leading to milk coagulation monitoring applications (Grassi, Alamprese, Bono, Casiraghi, & Amigo, 2014; Grassi et al., 2019; Lyndgaard, Engelsen, & van den Berg, 2012; Panikuttira, O'Shea, O'Donnell, & Tobin, 2017). In particular, among the chemometric tools, Multivariate Curve Resolution combined with Alternating Least Squares (MCR-ALS) is able to decompose the spectroscopic signal collected during NIR-based process monitoring into the contribution of several components with distinct spectral signatures, which are related to the different physicochemical forms of the product studied during the process development (De Juan & Tauler, 2006). MCR-ALS provides a bilinear model formed by chemically meaningful spectral signatures of the components, which can help in product characterization, and the related process concentration profiles, useful to interpret the time-dependent variation of the product forms. In difference with other chemometric tools, such as Principal Component Analysis (PCA) or Independent Component analysis (ICA), that provide bilinear models of few abstract profiles, MCR provides chemically meaningful profiles that can be more clearly interpreted and connected to the chemistry of the studied process; hence, the choice of this algorithm for this work (Parastar, Jalali-Heravi, & Tauler, 2012). The NIR/MCR-ALS combination meets the global dairy market need for sensor-based process monitoring and interpretation, which will necessarily increase process efficiency and improve product quality and yield (Pu, O'Donnell, Tobin, & O'Shea, 2020).

In this framework, the present work investigated the monitoring of the renneting phase of reconstituted milk obtained from different low and medium heat SMPs produced in different European countries. Coagulum formation was studied on unaltered reconstituted milk samples, pasteurized samples, samples with added calcium chloride and samples mixed with fresh liquid milk with the aim of evaluating the effect of the modifications in the raw reconstituted milk. Moreover, the potential ability of the combination NIR/MCR-ALS for the monitoring and understanding of cheesemaking process has been investigated foreseeing a suitable non-destructive, non-invasive and on-line tool to evaluate the rennet-induced coagulation of milks.

2. Materials and methods

2.1. Sample preparation

Six samples of SMP were recovered from wholesalers present on the Italian market and were compared to assess coagulation properties and to study the effect of added $CaCl_2$ on the progress of the coagulation process. The country of production and the characteristics of the products are shown in the first block of Table 1. SMPs were dissolved in 300 mL distilled water (24 °C) at nearly 10% (w/w) to yield reconstituted skim milk samples with the same protein content (3.4 ± 0.1 g/100 g). Complete powder dissolution was achieved by mixing with a magnetic stirrer bar at room temperature for 20 min. Some of these reconstituted milk samples were enriched with 1 (0.0035 g/L) or 0.5 (0.0018 g/L) mmol/L of $CaCl_2$, from a stock solution (50 g/L). After measuring the pH with a pH-meter 3627 (Mettler-Toledo, Columbus, OH, USA), the samples were divided in three subsamples of 100 mL each to be used for NIR monitoring, rheology and Formagraph tests. For each of these techniques, two technical replicates were analyzed.

Fresh milk samples and SMP samples from EPI (EPI ingredients, Nantes, France) and SCA (Società Coadiuvanti Alimentari, Piacenza,

Italy) milk were used to test the effect of pasteurization on milk coagulation, as shown in the second block of Table 1. Pasteurization was carried out at 73 °C for 16 s, by means of a self-assembled lab scale tubular heat exchanger.

A third study was oriented to test the effect of adding reconstituted milk (EPI and SCA powders) to fresh pasteurized milk (Granarolo, Bologna, Italy) on the coagulation process. Each reconstituted sample was mixed with skimmed milk in 40:60 and 60:40 ratios, as shown in the third block of Table 1. For these experiments, pasteurized skimmed milk and non-pasteurized skimmed milk were provided by CREA-ZA (Lodi, Italy) farm.

For all the coagulation trials, a concentration of 1.5 mL/L of liquid rennet (Naturen® 220 CHR Hansen, Hoersholm, Denmark) was used.

2.2. Formagraph analysis

The renneting properties were studied by using the Formagraph instrument (Foss Electric, Hillerød, Denmark). Milk samples were conditioned to 37 °C for 20 min before analysis, then rennet (Naturen® 220 CHR Hansen, Hoersholm, Denmark) was added at a final concentration of 0.088 IMCU/g of milk. Measurements of milk coagulation properties ended 60 min after the addition of the clotting enzyme. From the Formagraph curve, the rennet coagulation time (r, min) and curd firmness after 30 min (A_{30}, mm) were calculated.

2.3. Rheological measurements

Samples rheological behavior during renneting was studied by using a Physica MCR 102 rheometer (Anton Paar GmbH, Graz, Austria) supported with the software RheoCompass (v. 1.21, Anton Paar GmbH, Graz, Austria). Samples were heated in a thermostatic bath to 37 °C and the proper amount of rennet was added. Afterwards, 19 mL of sample were inserted in the preheated concentric cylinders (CC27) of the rheometer in order to start the analysis exactly 1 min after the rennet addition. A time curing test was performed at 37 °C applying a constant 0.1% strain at a fixed 1 Hz frequency, collecting data every 15 s for a total of 30 min.

2.4. FT-NIR spectroscopy

Rennet coagulation process of each sample, placed in a thermostatic bath at 37 °C, was continuously monitored for 30 min with a Fourier-Transform (FT)-NIR spectrometer (MPA, Bruker Optics, Milan, Italy). A fiber optic probe, equipped with a transflectance adapter with a 0.1 cm optical path (0.2 cm total effective pathlength), was inserted in the sample and spectra were collected every minute in the whole NIR spectral range, namely 12,500–4000 cm^{-1}, starting exactly 1 min after adding the liquid rennet. For each sample, 30 spectra were acquired, with a resolution of 8 cm^{-1} and 64 scans for both background and sample. OPUS software (v. 6.0 Bruker Optics, Milan, Italy) was used to manage the instrument.

2.5. Data analysis

Spectral, rheological and Formagraph data were processed and analyzed with toolboxes and routines present in Matlab environment (the Mathworks Inc. Natick, MA, USA).

The range of FT-NIR spectra was reduced to 12,500–5824 cm^{-1}, in order to remove spectral ranges with signal saturation and high noise. A toolbox (Jaumot, de Juan, & Tauler, 2015) implemented in Matlab was used to perform the MCR-ALS analysis on the spectra collected in each coagulation trial. The two technical replicates were not combined in a single multiset structure because the scattering was different in each run. Unlike other processes monitored with FT-NIR, scattering should not be removed by preprocessing in the coagulation process because it is an indication of the coagulation progress. Spectral data of each trial were arranged in a matrix $\boldsymbol{D}$ (MxN), where M are the number of spectra (30) and N the number of wavenumbers (1840). MCR-ALS decomposed each $\boldsymbol{D}$ matrix into two matrices: the concentration profiles $\boldsymbol{C}$ (MxF) and the spectral profiles $\boldsymbol{S^T}$ (FxN) matrices (Eq. (1)). The $\boldsymbol{S^T}$ matrix contains the spectral signatures of the F components linked to the different milk coagulation forms found during the monitored process, whereas the $\boldsymbol{C}$ matrix contains information about the evolution in time of the concentration of the F components during the process. Finally, $\boldsymbol{E}$ (MxN) is the matrix that contains the residuals.

$$\boldsymbol{D} = \boldsymbol{C}\boldsymbol{S^T} + \boldsymbol{E} \quad \text{(Eq. 1)}$$

Principal Component Analysis (PCA) was used prior to MCR-ALS in order to define the proper number of components (F) to describe the spectral variation recorded during the coagulation process. Next, the ALS optimization was started by using initial estimates of spectral profiles provided by a pure variable selection method based on SIMPLISMA (Windig & Stephenson, 1992). Once the initial estimates are obtained, $\boldsymbol{C}$ and $\boldsymbol{S^T}$ are alternatingly optimized in each iteration under the action of constraints. The constraints selected were non-negativity for the spectral and concentration profiles and unimodality, i.e. the presence of a single maximum per profile, in the concentration profiles because the different milk forms during the coagulation process can be considered to follow a kinetic sequential emergence-decay pattern. This procedure was similar to that followed in many process analysis examples (De Juan & Tauler, 2016; De Oliveira, Pedroza, Sousa, Lima, & de Juan, 2017; Grassi et al., 2014) and shows analogies with the study by Amigo, de Juan, Coello, and Maspoch (2006).

The calculation of $\boldsymbol{C}$ and $\boldsymbol{S^T}$ was repeated until a satisfactory reproduction of the original data $\boldsymbol{D}$ through the MCR model $\boldsymbol{CS^T}$ was achieved. In order to obtain satisfactory concentration and spectral profiles, a stopping convergence criterion was used based on the relative difference between percentages of lack of fit (LOF) between consecutive iterations:

$$LOF\ (\%) = 100^* \sqrt{\frac{\sum_{ij} e_{ij}^2}{\sum_{ij} d_{ij}^2}} \quad \text{(Eq. 2)}$$

where e_{ij} is each ijth component of the residual matrix ($\boldsymbol{E}$) and d_{ij} is each ijth component of $\boldsymbol{D}$ matrix. When the difference of two consecutive LOF percentages was lower than 0.1%, convergence was considered achieved and the iterative cycle stopped (Jaumot et al., 2015).

The modeling of the studied processes by MCR-ALS needed several components linked to the progress of the milk coagulation. The last concentration profile in time, linked to the coagulated form (called solid-like form in Grassi et al., 2014) was compared with rheological, after logarithmic transformation, and Formagraph curves, meant to describe the coagulation process as well. To do so, correlation coefficients among the three profiles (MCR, rheological and Formagraph curves) were calculated. Furthermore, the concentration profile linked to the coagulated form obtained from each MCR-ALS analysis was modelled as a function of coagulation time through the following sigmoid equation (Eq. (3)) implemented in Table Curve software (v. 4.0, Jandel Scientific, San Rafael, CA, USA) (Grassi et al., 2013):

$$Y = a^* exp\left\{ - exp\left[- \left(\frac{x - c ln(ln(2)) - b}{c} \right) \right] \right\} \quad \text{(Eq. 3)}$$

First and second derivatives of the MCR profile of the coagulated form were used to detect kinetic parameters characterizing the process,

i.e. the maximum acceleration, velocity and deceleration of each coagulation process. The maximum of first derivative of these curves was used to individuate the maximum speed of the process, whereas maximum and minimum of second derivatives were used to detect maximum acceleration and maximum deceleration of the process, respectively.

One-way analysis of variance (ANOVA) was performed to compare powder coagulation performance in term of r and A_{30}, calculated from the Formagraph curve, gelation point extrapolated from fundamental rheology analysis and maximum velocity of the solid-like concentration profile resulting from the MCR-ALS analysis. In case of statistically significant differences, a Least Significant Difference (LSD) post hoc test was performed.

3. Results and discussion

A clear increment of absorbance over time was observed during coagulation as shown in Fig. 1, due to scattering effects caused by suspended fat globules and micelles aggregation (Aernouts, Van Beers, Watté, Huybrechts, Lammertyn, & Saeys, 2015; Cabassi et al., 2013). Most of the changes occurs during the early moments of coagulation, especially in the 12500-9000 cm^{-1} region, where it is possible to observe a clear change in the spectra baseline overtime related to scattering effects linked to changes in particle size then on particle composition (Cabassi et al., 2013). The absorption band at 6900 cm^{-1} is ascribable to symmetric and asymmetric stretching of O–H water bond, whereas bands at 10,800 and 8600 are linked to C–H bonds of lipids (Tsenkova, Atanassova, Itoh, Ozaki, & Toyoda, 2000; Workman & Weyer, 2007).

According to the PCA results, all coagulation processes could be described with three spectral contributions. The initial estimates of MCR-ALS were selected using a pure variable detection method, which helped to select the three most different spectra of the dataset ***D***, in order to describe the process. The algorithm selected always the first and the last spectrum of each coagulation trial, whereas the other component was chosen at different processing times, depending on the considered conditions.

The application of the ALS procedure to the milk renneting trials

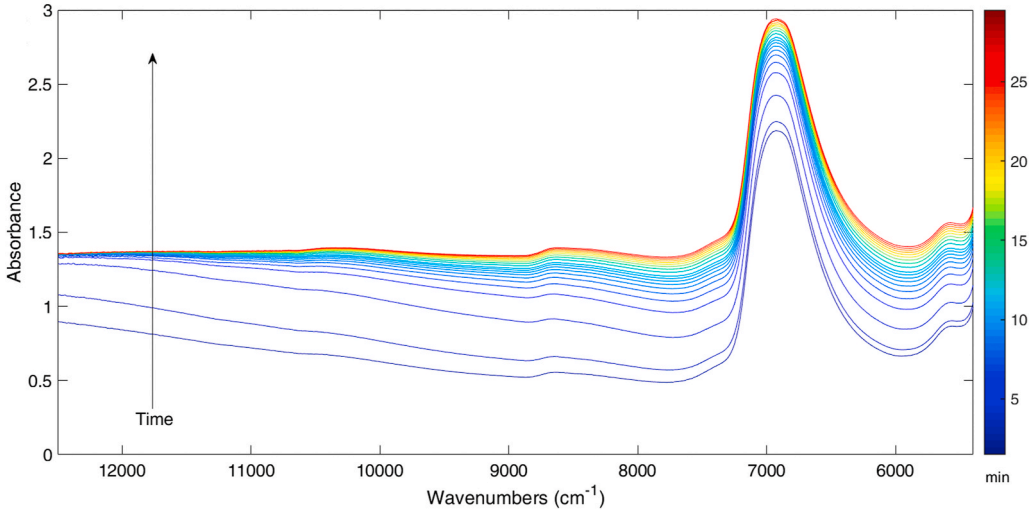

Fig. 1. Spectra collected during coagulation of the sample EPI 35. Legend refers to coagulation time (min).

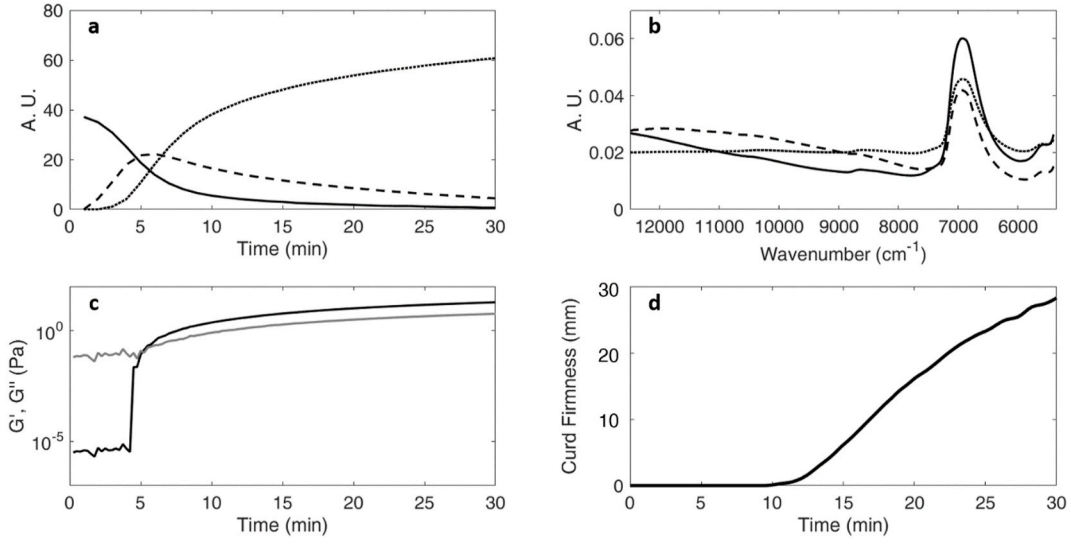

Fig. 2. Coagulation trial of the sample Rucker 35: MCR-ALS concentration (a) and spectral profiles (b) of liquid-like behaviour of milk (solid lines), transition phase (dashed lines) and solid-like behaviour of milk (dotted lines); (c) rheological data (black: G′, grey: G″); (d) Formagraph curve.

permitted the resolution of both concentration profiles (Fig. 2a) and pure spectra (Fig. 2b) of the milk forms involved. The obtained MCR-ALS models successfully described the process evolution. For all trials, the product CS^T explained more than 99.9% of variance of the data and the LOF was lower than 0.72%. Fig. 2a reports an example of concentration profiles for the coagulation performed with the sample Rucker 35. The obtained profiles contained information about the main changes occurring in milk. The first MCR-ALS concentration profile (represented by the solid line in Fig. 2a) had an inverse sigmoid shape in all the performed runs: it described the first stage of the rennet coagulation of milk, where rheological data showed low and constant G′ values (Fig. 2c) and curd firmness was equal to zero (Fig. 2d). This profile showed a clear decrease when the first aggregation of casein micelles caused a steep increase in the elasticity of the system, corresponding to the fast rise of G′ in the time curing curve (Fig. 2c). It is also interesting to note that, when the first concentration profile reached a null value, the Formagraph curve started to increase, meaning that liquid non-coagulated milk was almost absent. Thus, the first profile was associated to the liquid-like milk behavior. The third concentration profile (Fig. 2a, dotted line) had a sigmoid shape inversely correlated to the liquid-like behavior: the decreasing evolution of the first profile corresponded to the increasing evolution of the latter profile that confirmed the transition of milk from liquid to a viscoelastic structure, thus describing the milk solid-like behavior as already reported by Grassi et al. (2014) and Grassi et al. (2019). The transition profile (second concentration profile represented by the dashed line in Fig. 2a) reached its maximum at the time in which G′ crossed G'' (gelation point), due to the formation of a continuous protein network in the coagulated reconstituted milk. The observed differences in the time required to reach the maximum of the second profile were strictly related to the SMP used. The three pure spectra obtained in the MCR-ALS models (Fig. 2b) explained well the changes occurring in the FT-NIR data during the coagulation phases and confirmed what was previously found by Grassi et al. (2014) and Grassi et al. (2019). The solid line represented the typical spectrum recorded at the beginning of the renneting process, i.e. when the milk still had a liquid-like behavior. It showed a visible slope in the baseline at low wavenumbers and a high peak at 6900 cm^{-1} due to O–H combination band of symmetric and asymmetric stretching of water. The characteristic spectrum of coagulated milk, influenced by the characteristics of the continuous protein network, is represented by the dotted line and is characterized by an absence of slope between 12,500 and 7500 cm^{-1} and a reduction in the absorption of the peak at 6900 cm^{-1} if compared with the liquid-like behavior profile (solid line). The other pure spectrum (dashed line) stood for the transition phase, during which the first changes in the casein micelle structure took place, due to the solubilization of colloidal calcium phosphate. The relationship between casein coagulation and MCR-ALS profiles obtained by FT-NIR spectra analysis can be mainly ascribed to the spectra differences in baseline slope, caused by physical effects (Frake et al., 1998) such as the changes in number and size of casein micelles during rennet milk coagulation (Horne & Davidson, 1993), which are closely related to changes in light scattering. Furthermore, the significant reduction in the absorbance at 6900 cm^{-1} observed during renneting revealed the ability of the NIR probe of measuring the water retained by the curd, thus not poured out in the syneresis.

Similar behavior was obtained with all other coagulation experiments performed. The following subsections will address the study of different factors on the coagulation process based on different subsets of experiments as described in Table 1.

3.1. Effect of milk powder type and $CaCl_2$ on coagulation time

This study was carried out with the 12 samples of the first block in Table 1, considering different SMP types and $CaCl_2$ concentrations.

To better investigate the relationship between the MCR-ALS profiles and the reference tests (rheology and Formagraph), a correlation analysis was performed between MCR-ALS data and both Formagraph and rheological data (Table 2). In detail, the MCR-ALS solid-like behavior profile, the last one appearing in time, was correlated with G′, G″ and the Formagraph profile obtained for each coagulation trial.

The correlations between the concentration profiles related to the solid-like behavior and G′ and G″ curves were highly significant ($r > 0.92$; $p < 0.001$), with the exception of the trials performed with the two replicates of Lactalis 18 ($r < 0.80$), which were characterized by irregular coagulation profiles. However, correlations were significant in all cases, even for samples with lower correlation coefficient values. These results are in agreement with those by Klandar, Lagaude, and Chevalier-Lucia (2007), who also found highly significant correlations ($r > 0.83$, $p < 0.001$) between parameters obtained from G' curves and kinetic parameters derived from the time-dependent evolution of some absorbances at individual wavelengths in raw NIR spectra acquired on milk reconstituted from low-heat or medium-heat skim milk powders. Moreover, good correlations were found also between the MCR-ALS solid-like profiles and the Formagraph curves ($r > 0.88$, $p < 0.001$), especially for EPI ($r > 0.99$), Rucker ($r > 0.98$) and SCA ($r > 0.98$), the powders that presented the best coagulation properties. These results confirmed the significant correlation between MCR-ALS data and both the reference analyses taken into account, which in their turn, were well correlated among them (correlation coefficients between rheological and Formagraph curves were always higher than 0.92, $p < 0.001$, with the exception of trials performed with Lactalis 18).

Results of this block of experiments were used to select the best SMPs and $CaCl_2$ concentration in terms of speed of coagulum formation and strength. The characteristic indexes of the Formagraph analysis (A_{30} and r), the rheological gelation point (G′ and G″ cross-over) and the time corresponding to the maximum velocity (steepness) of the MCR-ALS solid-like behavior concentration profile, which was calculated from the maximum of the first derivative (Grassi et al., 2013), were calculated for all the performed trials and reported as the average of the two performed replicates (Table 3).

Table 2
Results of the correlation analysis between MCR-ALS milk solid-like concentration profile and rheological data (logG′ and logG'' curves) or Formagraph curve: correlation coefficients and statistical significance.

Sample ID	G′	G″	Formagraph
EPI 18 R1	0.99[a]	0.99[a]	0.99[a]
EPI 18 R2	0.99[a]	0.99[a]	0.99[a]
EPI 35 R1	0.99[a]	0.99[a]	0.99[a]
EPI 35 R2	0.99[a]	0.99[a]	0.99[a]
Lactalis 18 R1	0.75[a]	0.67[a]	0.99[a]
Lactalis 18 R2	0.73[a]	0.80[a]	0.99[a]
Lactalis 35 R1	0.93[a]	0.92[a]	0.97[a]
Lactalis 35 R2	0.92[a]	0.79[a]	0.97[a]
Rucker 18 R1	0.99[a]	0.98[a]	0.98[a]
Rucker 18 R2	0.99[a]	0.99[a]	0.99[a]
Rucker 35 R1	0.99[a]	0.98[a]	0.98[a]
Rucker 35 R2	0.99[a]	0.99[a]	0.98[a]
Safivo 18 R1	0.92[a]	0.97[a]	0.97[a]
Safivo 18 R2	0.96[a]	0.99[a]	0.97[a]
Safivo 35 R1	0.98[a]	0.98[a]	0.99[a]
Safivo 35 R2	0.99[a]	0.99[a]	0.99[a]
SCA 18 R1	0.99[a]	0.99[a]	0.99[a]
SCA 18 R2	0.99[a]	0.99[a]	0.99[a]
SCA 35 R1	0.99[a]	0.99[a]	0.98[a]
SCA 35 R2	0.99[a]	0.99[a]	0.98[a]
SIA 18 R1	0.95[a]	0.97[a]	0.99[a]
SIA 18 R2	0.97[a]	0.94[a]	0.99[a]
SIA 35 R1	0.99[a]	0.98[a]	0.88[a]
SIA 35 R2	0.99[a]	0.95[a]	0.88[a]

[a] $p < 0.001$; R1 = first replicate; R2 = second replicate.

Table 3
Characteristic indexes from Formagraph (A_{30} and r), fundamental rheology (gelation point) and MCR-ALS analysis (time corresponding to the maximum velocity of the concentration profile related to the solid-like behavior). In a column, results with the same letter are not statistically different between each other ($p > 0.05$).

	0.018 g/L of $CaCl_2$				0.035 g/L of $CaCl_2$			
Sample	A_{30} (mm)	r (min)	Gelation point (min)	Solid-like behavior concentration profile (max velocity, min)	A_{30} (mm)	r (min)	Gelation point (min)	Solid-like behavior concentration profile (max velocity, min)
EPI	42.1^{d}	8.0^{a}	2.0^{a}	3.9^{a}	39.6^{c}	10.1^{a}	2.3^{a}	4.2^{a}
Lactalis	10.8^{a}	17.5^{d}	–	10.4^{c}	11.9^{a}	18.2^{c}	–	8.9^{c}
Rucker	24.9^{b}	12.4^{b}	5.8^{b}	5.4^{b}	28.2^{b}	11.1^{a}	5.8^{b}	7.4^{b}
Safivo	11.8^{a}	16.8^{cd}	16.5^{c}	10.4^{c}	14.1^{a}	17.9^{c}	16.3^{c}	8.0^{c}
SCA	30.3^{c}	10.4^{ab}	5.0^{b}	6.5^{b}	31.2^{b}	13.1^{b}	4.8^{ab}	6.3^{ab}
SIA	16.1^{a}	15.4^{c}	7.5^{b}	–	16.1^{a}	16.1^{c}	6.3^{b}	5.7^{a}

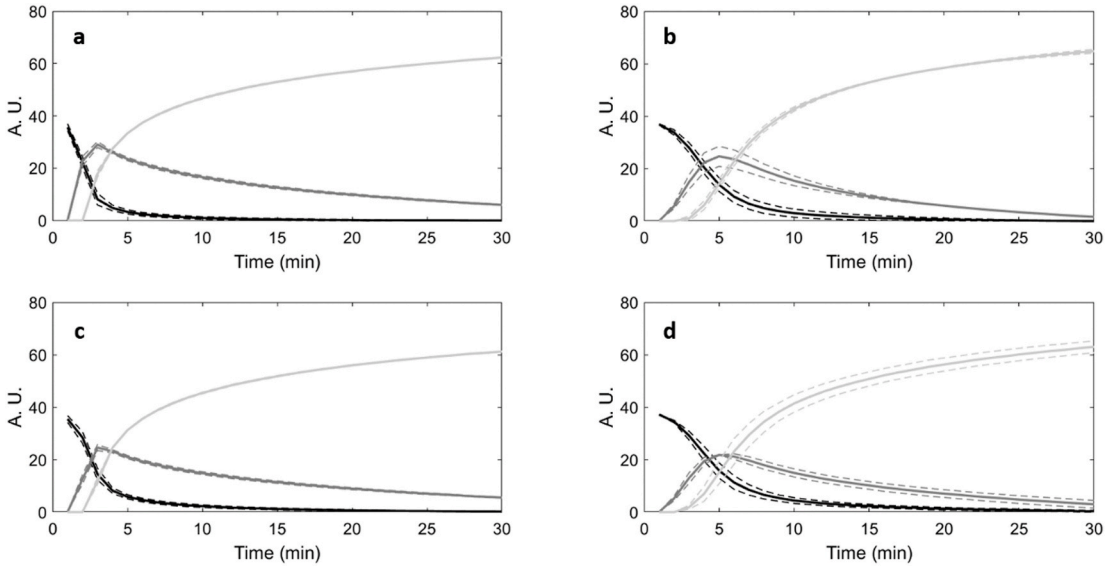

Fig. 3. MCR-ALS concentration profiles of EPI 18 (a), SCA 18 (b), Epi 35 (c) and SCA 35 (d) samples. Dashed lines represent standard deviation interval.

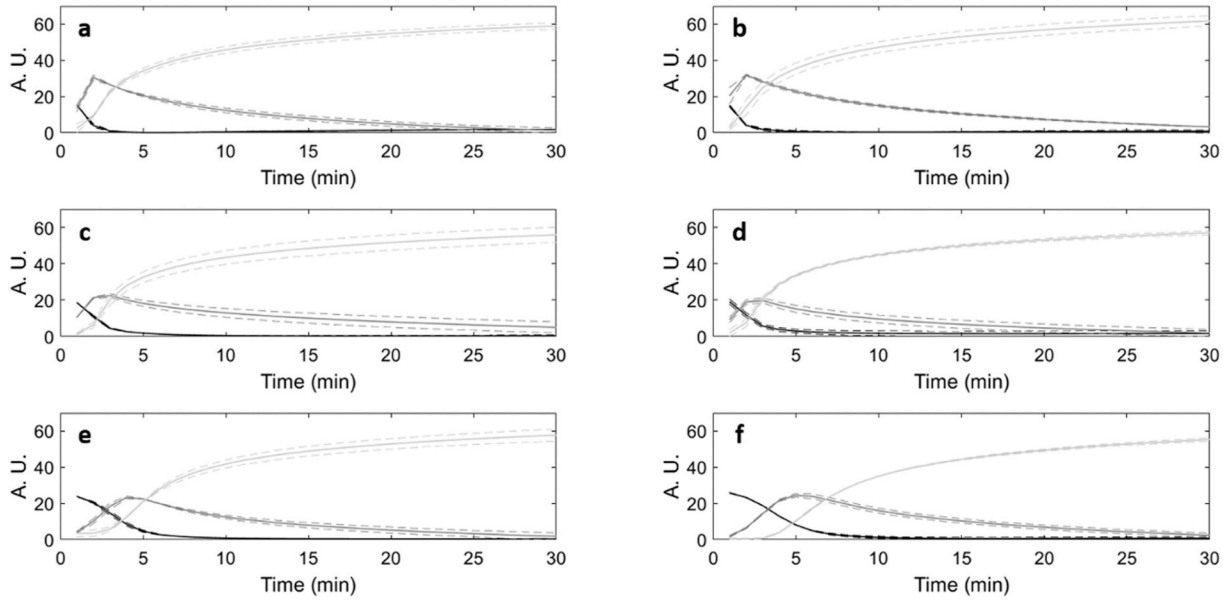

Fig. 4. MCR-ALS concentration profiles of renneting trials carried out with non-pasteurized skimmed milk (S NP) (a), pasteurized skimmed milk (S P) (b), non-pasteurized reconstituted EPI sample (EPI NP) (c), pasteurized reconstituted EPI sample (EPI P) (d), non-pasteurized reconstituted SCA sample (SCA NP) (e) and pasteurized reconstituted SCA sample (SCA P) (f). Dashed lines represent standard deviation interval.

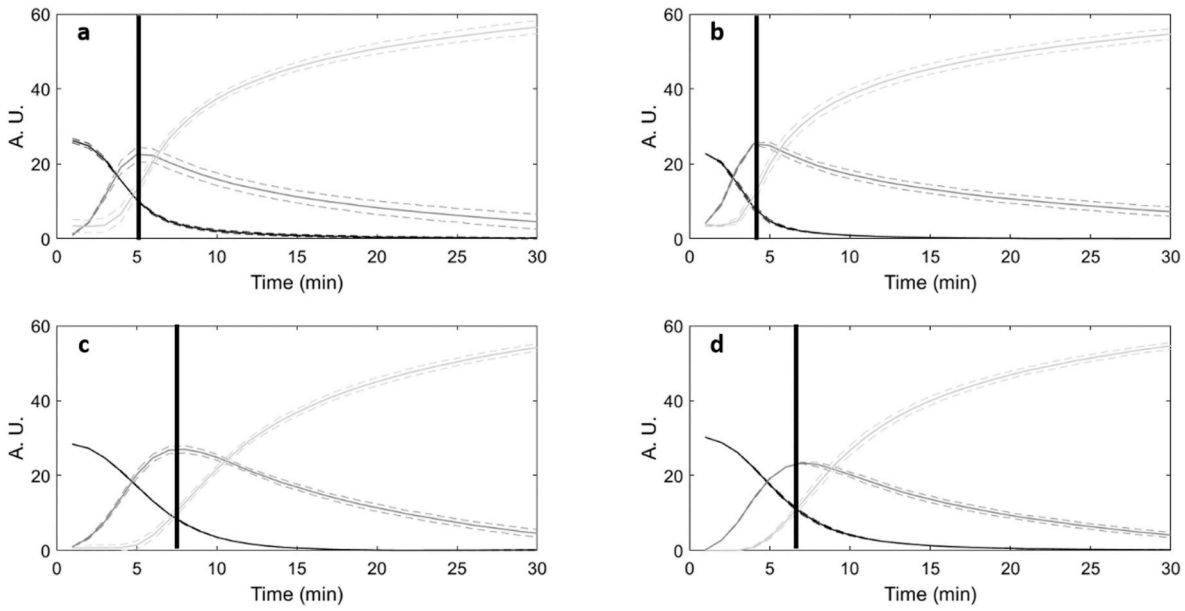

Fig. 5. MCR-ALS concentration profiles of coagulation trials performed with the mixtures of pasteurized skimmed milk and reconstituted milk samples: EPI 40 (a), EPI 60 (b), SCA 40 (c) and SCA 60 (d). Dashed lines represent standard deviation interval.

EPI and SCA resulted the best powders for milk enrichment as the A_{30} values were significantly higher ($p < 0.05$) than those obtained for the other SMPs; furthermore, the coagulation of reconstituted EPI and SCA milk samples occurred faster ($r < 10.5$ min, gelation point < 5 min). The times corresponding to the maximum velocity of the milk solid-like concentration profile agreed with Formagraph and rheological results, confirming the optimal behavior of the reconstituted powders in terms of coagulation occurrence.

The MCR-ALS analysis, in agreement with Formagraph and rheological data, showed that the concentration of calcium chloride did not significantly affect the coagulation process. Indeed, in Fig. 3 it is possible to visually confirm that there was no difference between EPI 18 (Fig. 3a) and EPI 35 (Fig. 3c) samples nor between SCA 18 (Fig. 3b) and SCA 35 (Fig. 3d) samples, since the maxima of the transition concentration profiles (dark grey) occurred at the same time.

Based on these results, EPI and SCA were selected as the best powders in terms of coagulation properties and used for further analyses. Considering the good agreement of the information obtained from rheological and Formagraph curves and MCR-ALS profiles issued from FT-NIR data, the second block of experiments were carried out using only FT-NIR monitoring (much faster) and MCR-ALS.

3.2. Effect of pasteurization in coagulation

To evaluate the possible effect of pasteurization on coagulation properties, six different coagulation trials were performed in duplicate using skimmed milk and EPI and SCA reconstituted samples, both non-pasteurized and pasteurized, maintaining the $CaCl_2$ concentration at 0.035 g/L (see second block in Table 1). As shown in Fig. 4, in which the three MCR-ALS concentration profiles of all the trials are reported, there were no substantial differences between non-pasteurized and pasteurized samples, except for SCA P (Fig. 4f), whose coagulation appeared slightly delayed (1 min) with respect to SCA NP sample (Fig. 4e). The delay could be linked to thermally induced changes in milk proteins, indeed SCA is a medium-heat SMP and a pasteurization procedure could influence the already modified interactions among caseins and denatured whey proteins (Kethireddipalli & Hill, 2015) causing a light delay in the coagulation.

3.3. Effect of addition of reconstituted milk to fresh milk samples on coagulation

MCR-ALS was also applied to spectral data collected during the coagulation trials of pasteurized skimmed milk mixed with reconstituted milk samples. Both EPI and SCA reconstituted samples were mixed with 40% and 60% of pasteurized skimmed milk, and each experiment was replicated three times, for a total of twelve trials (third block in Table 1). The results (Fig. 5) highlighted that a lower amount of reconstituted milk in the mixture corresponded to a delayed occurrence of the coagulum formation (indicated in the figure by the black vertical lines). In fact, in samples containing 60% of reconstituted milk (Fig. 5b and d) the peak of the transition concentration profiles occurred 1–2 min earlier than the ones of the samples with 40% reconstituted milk (Fig. 5a and c). In the experiments performed, the higher the amount of powder used, the faster the coagulum occurrence, approaching the performance of pasteurized skimmed milk (Fig. 4b) when 100% of reconstituted milk was used (Fig. 4d and f). Indeed, the maximum of the transition profiles recorded for the pasteurized skimmed milk occurred around 2 min, for reconstituted EPI and SCA samples (EPI P, SCA P) occurred at around 2 and 5 min (Fig. 4d and f), for EPI 60 and SCA 60 at 4.3 and 6.6 min, and for EPI 40 and SCA 40 at 5.3 and 8.1 min (Fig. 5), respectively.

4. Conclusions

A wide range of experimental conditions were studied in order to describe the coagulation process and the possible changes undergone due to different low and medium heat skim milk powders, amount of $CaCl_2$ added, use of pasteurization treatment and fraction of recon-

stituted milk powders.

MCR-ALS combined with FT-NIR monitoring during milk coagulation process was proposed as an alternative to standard methods, such as Formagraph and rheological methods. The process profile of the coagulated milk form obtained with the developed approach, highly correlated to the standard methods (always $r > 0.67$, and for the powders with the best coagulation properties $r > 0.98$, $p < 0.001$), allowed proving the significant effect of the milk powder type on coagulation occurrence, as opposed to the non-significance of the added $CaCl_2$ concentration and the heat treatment. Moreover, monitoring of coagulation trials of pasteurized skimmed milk mixed with reconstituted milk samples permitted the identification of shorter coagulation times when higher reconstituted milk percentage was used.

Profiles extracted from MCR-ALS models appear to be suitable as a fast, non-destructive, non-invasive on-line method to evaluate the rennet-induced coagulation of reconstituted milks and to assess changes in coagulation performance for a wide range of coagulation conditions.

CRediT authorship contribution statement

Lorenzo Strani: Conceptualization, Methodology, Software, Formal analysis, Data curation, Writing - original draft. **Silvia Grassi:** Conceptualization, Methodology, Data curation, Writing - original draft. **Cristina Alamprese:** Conceptualization, Methodology, Supervision, Writing - original draft. **Ernestina Casiraghi:** Conceptualization, Supervision. **Roberta Ghiglietti:** Methodology, Formal analysis, Writing - original draft. **Francesco Locci:** Methodology, Formal analysis, Writing - original draft. **Nicolò Pricca:** Methodology, Writing - original draft. **Anna De Juan:** Supervision, Software, Data curation, Writing - original draft.

Declaration of competing interest

The authors declare that they have no known competing financial interests or personal relationships that could have appeared to influence the work reported in this paper.

Acknowledgements

The authors would like to thank Dr. Giovanni Cabassi of CREA-ZA, Research Centre for Animal Production and Aquaculture (via A. Lombardo 11, 26900 Lodi, Italy) for his helpful suggestions. A.J. thanks support from the Spanish government through the research project PID 2019-1071586B-IOO.

References

Aernouts, B., Van Beers, R., Watté, R., Huybrechts, T., Lammertyn, J., & Saeys, W. (2015). Visible and near-infrared bulk optical properties of raw milk. *Journal of Dairy Science, 98*(10), 6727–6738.

Amigo, J. M., de Juan, A., Coello, J., & Maspoch, S. (2006). A mixed hard-and soft-modelling approach to study and monitor enzymatic systems in biological fluids. *Analytica Chimica Acta, 567*(2), 245–254.

Cabassi, G., Profaizer, M., et al. (2013). Estimation of fat globule size distribution in milk using an inverse light scattering model in the near infrared region. *Journal of Near Infrared Spectroscopy, 21*(5), 359–373.

De Juan, A., & Tauler, R. (2006). Multivariate curve resolution (MCR) from 2000: Progress in concepts & applications. *Critical Reviews in Analytical Chemistry, 36*, 163–176.

De Juan, A., & Tauler, R. (2016). Multivariate curve resolution-alternating least squares for spectroscopic data. In *Data handling in science and technology* (pp. 5–51). Amsterdam, Netherlands: Elsevier.

De Oliveira, R. R., Pedroza, R. H., Sousa, A. O., Lima, K. M., & de Juan, A. (2017). Process modeling and control applied to real-time monitoring of distillation processes by near-infrared spectroscopy. *Analytica Chimica Acta, 985*, 41–53.

Frake, P., Luscombe, C. N., Rudd, D. R., Gill, I., Waterhouse, J., & Jayasooriya, U. A. (1998). Near-infrared mass median particle size determination of lactose monohydrate, evaluating several chemometric approaches. *Analyst, 123*(10), 2043–2046.

Gastaldi, E., Pellegrini, O., Lagaude, A., & de la Fuente, B. T. (1994). Functions of added calcium in acid milk coagulation. *Journal of Food Science, 59*(2), 310–312.

Grassi, S., Alamprese, C., Bono, V., Casiraghi, E., & Amigo, J. M. (2014). Modelling milk lactic acid fermentation using multivariate curve resolution-alternating least squares (MCR-ALS). *Food and Bioprocess Technology, 7*, 1819–1829.

Grassi, S., Alamprese, C., Bono, V., Picozzi, C., Foschino, R., & Casiraghi, E. (2013). Monitoring of lactic acid fermentation process using Fourier transform near infrared spectroscopy. *Journal of Near Infrared Spectroscopy, 21*(5), 417–425.

Grassi, S., Strani, L., Casiraghi, E., & Alamprese, C. (2019). Control and monitoring of milk renneting using FT-NIR spectroscopy as a Process Analytical Technology tool. *Foods, 8*(9), 405.

Gulati, A., Hennessy, D., O'Donovan, M., McManus, J. J., Fenelon, M. A., & Guinee, T. P. (2019). Dairy cow feeding system alters the characteristics of low-heat skim milk powder and processability of reconstituted skim milk. *Journal of Dairy Science, 102*(10), 8630–8647.

Han, Y., Mei, Y., Li, K., Xu, Y., & Wang, F. (2019). Effect of transglutaminase on rennet-induced gelation of skim milk and soymilk mixtures. *Journal of the Science of Food and Agriculture, 99*(4), 1820–1827.

Horne, D. S., & Davidson, C. M. (1993). Direct observation of decrease in size of casein micelles during the initial stages of renneting of skim milk. *International Dairy Journal, 3*(1), 61–71.

IDF. (2019). *Applications of near infrared spectrometry for the analysis of milk and milk products. IDF 497:2019*. Brussel, Belgium: International Dairy Federation.

Jaumot, J., de Juan, A., & Tauler, R. (2015). MCR-ALS GUI 2.0: New features and applications. *Chemometrics and Intelligent Laboratory Systems, 140*, 1–12.

Kern, C., Bähler, B., Hinrichs, J., & Nöbel, S. (2019). Waterless single screw extrusion of pasta-filata cheese: Process design based on thermo-rheological material properties. *Journal of Food Engineering, 260*, 58–69.

Kethireddipalli, P., & Hill, A. R. (2015). Rennet coagulation and cheesemaking properties of thermally processed milk: Overview and recent developments. *Journal of Agricultural and Food Chemistry, 63*(43), 9389–9403.

Kjaergaard-Jansen, G. (1990). Milk powders: Specification in relation to the products to be manufactures. In *Recombination of milk and milk products, Special Issue No. 9001* (pp. 104–125). Brussel, Belgium: International Dairy Federation.

Klandar, A. H., Lagaude, A., & Chevalier-Lucia, D. (2007). Assessment of the rennet coagulation of skim milk: A comparison of methods. *International Dairy Journal, 17*(10), 1151–1160.

Lelievret, J., Shaker, R. R., & Taylor, M. W. (1991). The influence of milk powder characteristics on the properties of halloumi cheese made from recombined milk. *International Journal of Dairy Technology, 44*(2), 41–45.

Lin, Y., Kelly, A. L., O'Mahony, J. A., & Guinee, T. P. (2017). Addition of sodium caseinate to skim milk increases nonsedimentable casein and causes significant changes in rennet-induced gelation, heat stability, and ethanol stability. *Journal of Dairy Science, 100*(2), 908–918.

Lucey, J. A., Gorry, C., & Fox, P. F. (1994). Methods for improving the rennet coagulation properties of heated milk. In *IDF seminar. Cheese yield and factors affecting its control, Cork (Ireland), Apr 1993*. Brussel, Belgium: International Dairy Federation.

Lyndgaard, C. B., Engelsen, S. B., & van den Berg, F. W. (2012). Real-time modeling of milk coagulation using in-line near infrared spectroscopy. *Journal of Food Engineering, 108*(2), 345–352.

Marinoni, L., Monti, L., Barzaghi, S., & de la Roza-Delgado, B. (2013). Quantification of casein fractions and of some of their genetic variants in phosphate buffer by near infrared spectroscopy. *Journal of Near Infrared Spectroscopy, 21*(5), 385–394.

Nassar, K. S., Lu, J., Pang, X., Ragab, E. S., Yue, Y., Zhang, S., et al. (2020). Rheological and microstructural properties of rennet gel made from caprine milk treated by HP. *Journal of Food Engineering, 267*, 109710.

Omar, M. M., & Buchheim, W. (1983). Composition and microstructure of soft brine cheese made from instant whole milk powder. *Food Structure, 2*(1), 6.

O'Callaghan, D. J., O'Donnell, C. P., & Payne, F. A. (2002). Review of systems for monitoring curd setting during cheesemaking. *International Journal of Dairy Technology, 55*(2), 65–74.

Panikuttira, B., O'Shea, N., O'Donnell, C. P., & Tobin, J. T. (2017). PAT approach for cheese manufacture. *TResearch, 12*, 24–25.

Papadatos, A., Berger, A. M., Pratt, J. E., & Barbano, D. M. (2002). A nonlinear programming optimization model to maximize net revenue in cheese manufacture. *Journal of Dairy Science, 85*(11), 2768–2785.

Parastar, H., Jalali-Heravi, M., & Tauler, R. (2012). Is independent component analysis appropriate for multivariate resolution in analytical chemistry? *TRAC Trends in Analytical Chemistry, 31*, 134–143.

Písecký, J. (2005). Spray drying in the cheese industry. *International Dairy Journal, 15*(6–9), 531–536.

Pretto, D., Kaart, T., Vallas, M., Jõudu, I., Henno, M., Ancilotto, L., et al. (2011). Relationships between milk coagulation property traits analyzed with different methodologies. *Journal of Dairy Science, 94*(9), 4336–4346.

Pu, Y. Y., O'Donnell, C., Tobin, J. T., & O'Shea, N. (2020). Review of near-infrared spectroscopy as a process analytical technology for real-time product monitoring in dairy processing. *International Dairy Journal, 103*, 104623.

Rynne, N. M., Beresford, T. P., Kelly, A. L., & Guinee, T. P. (2004). Effect of milk pasteurization temperature and in situ whey protein denaturation on the composition, texture and heat-induced functionality of half-fat Cheddar cheese. *International Dairy Journal, 14*(11), 989–1001.

Salvador, D., Arango, O., & Castillo, M. (2019). In-line estimation of the elastic module of milk gels with variation of temperature protein concentration. *International Journal of Food Science and Technology, 54*(2), 354–360.

Sandra, S., Ho, M., Alexander, M., & Corredig, M. (2012). Effect of soluble calcium on the renneting properties of casein micelles as measured by rheology and diffusing wave spectroscopy. *Journal of Dairy Science, 95*(1), 75–82.

Singh, H., & Waungana, A. (2001). Influence of heat treatment of milk on cheesemaking properties. *International Dairy Journal, 11*(4–7), 543–551.
Strani, L., Grassi, S., Casiraghi, E., Alamprese, C., & Marini, F. (2019). Milk Renneting: Study of process factor influences by FT-NIR spectroscopy and chemometrics. *Food and Bioprocess Technology, 12*(6), 954–963.
Tsenkova, R., Atanassova, S., Itoh, K., Ozaki, Y., & Toyoda, K. (2000). Near infrared spectroscopy for biomonitoring: Cow milk composition measurement in a spectral region from 1,100 to 2,400 nanometers. *Journal of Animal Science, 78*(3), 515–522.
Udabage, P., McKinnon, I. R., & Augustin, M. A. (2000). Mineral and casein equilibria in milk: Effects of added salts and calcium-chelating agents. *Journal of Dairy Research, 67*(3), 361–370.
Windig, W., & Stephenson, D. A. (1992). Self-modeling mixture analysis of second-derivative near-infrared spectral data using the SIMPLISMA approach. *Analytical Chemistry, 64*(22), 2735–2742.
Workman, J., & Weyer, L. (2007). *Practical guide to interpretive near-infrared spectroscopy*. Boca Raton: CRC Press.

Further reading

Kelly, A. L., & Fox, P. F. (2016). Manufacture and properties of dairy powders. In *Advanced dairy chemistry* (pp. 1–33). New York, USA: Springer.